Chemical Engineering Journal 352 (2018) 277–282

Contents lists available at ScienceDirect

Chemical Engineering Journal

journal homepage: www.elsevier.com/locate/cej

Machine learning meets continuous flow chemistry: Automated optimization towards the Pareto front of multiple objectives

Artur M. Schweidtmann[a,b], Adam D. Clayton[c], Nicholas Holmes[c], Eric Bradford[a,d], Richard A. Bourne[c,*], Alexei A. Lapkin[a,*]

[a] Department of Chemical Engineering and Biotechnology, University of Cambridge, Cambridge CB3 0AS, UK
[b] Aachener Verfahrenstchnik, Process Systems Engineering, RWTH Aachen University, Aachen, Germany
[c] Institute of Process Research and Development, School of Chemistry & School of Chemical and Process Engineering, University of Leeds, Leeds LS2 9JT, UK
[d] Department of Engineering Cybernetics, NTNU University, Trondheim, Norway

HIGHLIGHTS

- Multi-objective algorithm applied to the self-optimization of flow reactor.
- Algorithm simultaneously targeted reactor productivity and environmental objectives.
- Pareto front shows the trade-off between these target objectives.
- Gaussian process models provide knowledge about the nature of interactions.

GRAPHICAL ABSTRACT

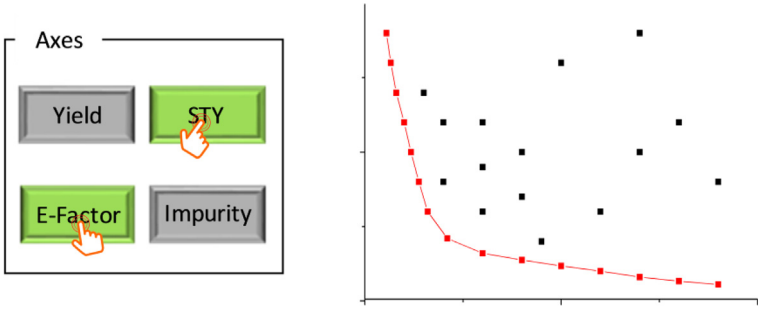

ARTICLE INFO

Keywords:
Automated flow reactor
Environmental chemistry
Machine learning
Reaction engineering
Sustainable chemistry

ABSTRACT

Automated development of chemical processes requires access to sophisticated algorithms for multi-objective optimization, since single-objective optimization fails to identify the trade-offs between conflicting performance criteria. Herein we report the implementation of a new multi-objective machine learning optimization algorithm for self-optimization, and demonstrate it in two exemplar chemical reactions performed in continuous flow. The algorithm successfully identified a set of optimal conditions corresponding to the trade-off curve (Pareto front) between environmental and economic objectives in both cases. Thus, it reveals the complete underlying trade-off and is not limited to one compromise as is the case in many other studies. The machine learning algorithm proved to be extremely data efficient, identifying the optimal conditions for the objectives in a lower number of experiments compared to single-objective optimizations. The complete underlying trade-off between multiple objectives is identified without arbitrary weighting factors, but via true multi-objective optimization.

1. Introduction

Robotic automated chemistry development is the future of chemistry and chemical manufacturing – increasingly methods using robotics and machine learning are applied to discovering new chemical transformations [1], synthesizing organic compounds [2], and multiple process parameter optimization [3–5]. The task of optimizing chemical reactions is highly challenging, since optimization response surfaces are often non-linear, and there are many simultaneous objective functions, such as reaction yield, process cost, impurity levels and environmental

* Corresponding authors.
E-mail addresses: r.a.bourne@leeds.ac.uk (R.A. Bourne), aal35@cam.ac.uk (A.A. Lapkin).

https://doi.org/10.1016/j.cej.2018.07.031
Received 11 April 2018; Received in revised form 2 July 2018; Accepted 3 July 2018
Available online 04 July 2018

impact, which need to be considered [6]. Especially the problem of optimizing the impurities profile is of huge significance for the pharmaceutical industry. The ability to perform efficient and automated multi-objective optimization represents a step-change advance in developing novel chemical processes. However, in the optimization community, the problem of multi-objective black-box optimization where the objective functions are expensive-to-evaluate, in terms of cost and time of conducting an experiment, which covers most problems of interest to the chemistry community, belongs to the class of 'orphan' problems, with very few advanced algorithms available. This paper demonstrates for the first time the use of true multi-objective machine learning methods for the self-optimization of two exemplar chemical reactions with competing economic and environmental objectives. We demonstrate that both objectives can be simultaneously optimized and that a set of optimal solutions corresponding to the trade-off between reactor productivity and environmental impact can be identified. Furthermore, the problem of minimizing product impurities was included, which has not been addressed in previous self-optimizations [7–12].

Single-objective optimization algorithms, such as simplex [13,14] and SNOBFIT [15], have been successfully employed for the optimization of chemical reactions [16–23]. However, it is important to consider multiple performance criteria when developing a chemical process. For example, Moore and Jensen observed low conversion at the self-optimized conditions corresponding to optimal productivity for a Paal-Knorr reaction, thus yielding an overall sub-optimal process. This was resolved by the addition of a penalty term for low conversion to their objective function [24].

The combination of multiple competing objectives into a single function is a common remedy. This was demonstrated by Houben et al. for the multitarget optimization of an emulsion polymerization process using a machine learning algorithm [25,26]. However, the *a priori* determination of adequate weights for these objectives is difficult. For example, Fitzpatrick et al. combined throughput, conversion and consumption into a single-objective function that led to skewed results [27].

These examples highlight two major problems with the scalarization of multiple performance criteria: (i) quantitative *a priori* knowledge is needed which requires additional experiments; (ii) only one optimal result is obtained which is dependent on the chosen objective function and does not reveal the complete trade-off between multiple performance criteria, i.e., their Pareto front (Fig. 1).

As economic and environmental objectives are generally competing, it is impossible to find one point where both objectives are at their optimal values [6]. Rather, the solution of a multi-objective optimization problem is a set of non-dominated points where one objective cannot be improved without having a detrimental effect on the other. This set is called a Pareto front (Fig. 1) [28]. The goal of this study is to explore the complete Pareto front of a reaction system and not only a single compromise point. This requires the simultaneous optimization of multiple objectives.

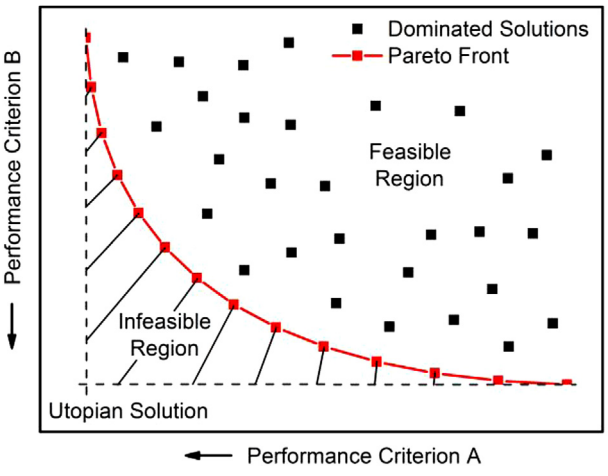

Fig. 1. An example of a system with two competing minimization performance criteria A and B. It is infeasible to find the utopian point where both A and B are at their optimal values. The points on the Pareto front are non-dominated solutions, as A or B cannot be improved without having a detrimental effect on the other.

Multiple (conflicting) objectives are encountered in many chemical engineering applications, e.g., conversion and selectivity in a chemical reaction [29]. The simultaneous optimization of those using multi-objective optimization techniques has also been reported in numerous literature examples [30–35]. As solution strategies, parametric approach, epsilon constraint method or genetic algorithms like the NSGA-II algorithm are most commonly used [36]. However, these methods are not well-suited for the automated chemical reaction system because they require many function evaluations and partly derivative information that is not (analytically) available.

Bayesian optimization methods are derivative-free global stochastic optimization methods that are particularly well-suited for expensive-to-evaluate problems. They have successfully been used to optimize expensive-to-evaluate computer simulations in many disciplines [35,37–39]. To archive this, Bayesian optimization algorithms train Gaussian process (GP) surrogate models on available data and identify new samples based on the predictions and uncertainty of the surrogates.

There exist a few multi-objective Bayesian optimization algorithms that aim to approximate a Pareto front, including: Thompson Sampling Efficient Multi-Objective (TS-EMO) [40–42], ParEGO [43] and expected hypervolume improvement (EHI) [44]. The quality of a Pareto front can be quantified by its hypervolume, i.e., the area spanned by the Pareto front and a reference point in the 2-dimensional case. Data efficiency in this context is given by hypervolume obtained in a limited number of function evaluations. In this work, we use TS-EMO which has been shown to have comparable or better data efficiency than both EHI and ParEGO. Further, TS-EMO has performed favorable compared to the commonly used genetic algorithm NSGA-II on a set of mathematical test functions for a given budget [40–42]. The TS-EMO algorithm [40–42] has recently been applied to the optimization of a process flowsheet, combining targets of low cost and low carbon emissions over the life cycle [35]. An open-source implementation of TS-EMO is available on GitHub [42].

2. Results and discussion

Herein, the recently developed TS-EMO algorithm is combined with an automated continuous reaction system. A small dataset is collected using Latin hypercube (LHC) sampling to initialize the TS-EMO algorithm [45,46]. Within the algorithm, individual GP surrogate models are trained to approximate the unknown response surfaces of the objectives [46,47]. The GPs are non-parametric regression models that can be understood as infinite dimensional generalizations of multivariate Gaussian distributions [46]. The TS-EMO algorithm randomly samples functions from those GPs using spectral sampling. Then, a multi-objective genetic algorithm is called within TS-EMO and identifies the Pareto front of the random samples. Finally, TS-EMO identifies a set of experiments from that Pareto front (of the random GP samples), which aim to improve the hypervolume of the actual Pareto front (of the experiments conducted). After conducting the suggested experiments, the GPs are updated and the process is repeated iteratively for a desired number of experiments. Within the algorithm the randomness of sampling naturally accounts for the exploration and exploitation trade-off desired in Bayesian optimization.

The TS-EMO algorithm was incorporated into the automated flow reactor (Scheme 1) and evaluated using two case studies: (i) S_NAr reaction between 2,4-difluoronitrobenzene **1** and morpholine **2** to form desired *ortho* product **3** and undesired *para*-**4** and bis adduct **5** (Scheme

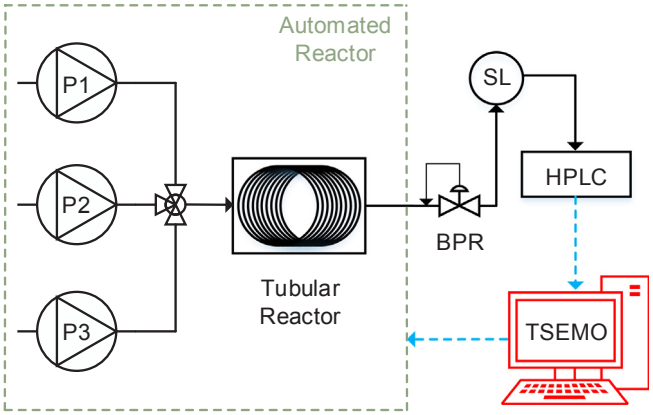

Scheme 1. Reactor set-up for case studies. Reagents were pumped using JASCO PU980 pumps (P) and were mixed in Swagelok tee-pieces. A Polar Bear Plus Flow Synthesiser was used for heating and cooling of the tubular reactor. Aliquots of the reaction mixture were delivered to the HPLC mobile phase using a VICI Valco 4 port sample loop (SL). The reaction was maintained under fixed back pressure using an Upchurch Scientific back pressure regulator (BPR). PTFE tubing (1/16″ OD, 1/32″ ID) provided by Polyflon was used throughout the reactor. Swagelok unions and fittings were used throughout apart from the sample loop (VICI) and BPR (Upchurch). Quantitative analysis was performed on an Agilent 1100 series HPLC instrument. The automated reactor was controlled by a custom written Matlab program, within which the TSEMO algorithm was implemented. See ESI for more experimental details.

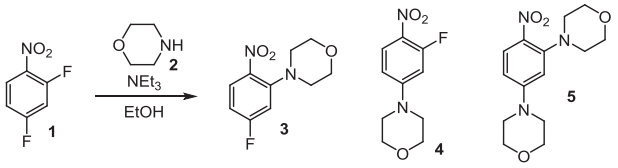

Scheme 2. Case study one: S_NAr reaction.

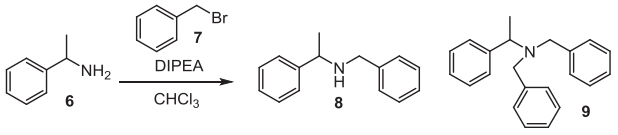

Scheme 3. Case study two: *N*-benzylation reaction.

2); [47] (ii) *N*-benzylation of α-methylbenzylamine **6** with benzyl bromide **7** to form desired 2° amine **8** and undesired 3° amine **9** (Scheme 3) [48]. In both cases, the product composition was determined by on-line HPLC and the data used as inputs for the TS-EMO algorithm.

To find environmentally acceptable and economic operating conditions for the synthesis of *ortho*-**3**, we aimed to maximize the space-time yield (STY) and minimize the E-factor of the reaction simultaneously [Eq. (1)], where the STY is a measure of reactor productivity [Eq. (2)] and the E-factor is defined as the ratio of the mass of waste to the mass of product [Eq. (3)] [49].

$$\text{minimize}\,[-\ln(\text{STY}),\ \ln(\text{E-factor})] \tag{1}$$

$$\text{STY} = \dot{m}_{\text{product}}/(V \times t_{res}) \tag{2}$$

$$\text{E-factor} = \dot{m}_{\text{waste}}/\dot{m}_{\text{product}} \tag{3}$$

where $\dot{m}_{\text{product}}$ = mass of product, $\dot{m}_{\text{waste}}$ = mass of waste, V = volume of reactor and t_{res} = residence time.

It is important to note that the product composition, and the resulting downstream processes (work-up etc.), will have a significant impact on the STY and E-factor of a process. However, such considerations were beyond the scope of this work, as non-reactive unit operations were not included in the optimizations.

Table 1
Optimization limits for the self-optimizations. Reservoir solutions: **1** = 2.0 M in EtOH; **2** = 4.2 M in EtOH; **6** = 0.4 M in $CHCl_3$; **7** = 0.4 M in $CHCl_3$.

Case Study One: S_NAr Reaction				
Limits	t_{res}/min	Morpholine/eq	Conc **1**/M	Temp/°C
Lower	0.5	1.0	0.1	60
Upper	2.0	5.0	0.5	140
Case Study Two: *N*-benzylation[a]				
Limits	**6**/mL min^{-1}	**7**:**6**	Solvent:**6**	Temp/°C
Lower	0.2	1.0	0.5	110
Upper	0.4	5.0	1.0	150

[a] Optimization parameters directly input in terms of flow rates and ratios. **7**:**6** is related to the benzyl bromide **7** equivalents and solvent:**6** is related to the concentration of **6**.

The objectives were natural log-transformed as this is known to enhance response-surface-based optimization [50]. Due to the log-transformation, the distances in the Pareto front of the algorithm are log-scaled and hence the algorithm favors a log-spaced Pareto front. The optimization was conducted with respect to four-variables: residence time (t_{res}), morpholine **2** equivalents, concentration of **1** and temperature (Table 1). The results of the optimization are shown in Fig. 2.

Herein, the automated setup was started in the evening and run overnight. The algorithm was terminated manually in the morning under the criterion that a dense front of at least 20 experimental Pareto data points were collected. The initial LHC size was 20, and results were in the region of solutions corresponding to high E-factors and low STYs. Nevertheless, the subsequent 48 experiments designed by the TS-EMO algorithm rapidly converged to a dense Pareto front consisting of 26 points. The optimal STY was 13,120 kg m^{-3} h^{-1} with an E-factor of 1.6. Conversely, the optimal E-factor was 0.2 with a STY of 3650 kg m^{-3} h^{-1}. Therefore, the data shows the inherent trade-off between STY and E-factor. The Pareto front can be divided into two sections. The left section where the gradient is shallow, the STY can be significantly increased whilst having a relatively small effect on the E-factor. This corresponds to decreasing the t_{res} at the lower limit of morpholine equivalents. The STY can be further improved by increasing the morpholine equivalents at the lower t_{res} limit. However, this results

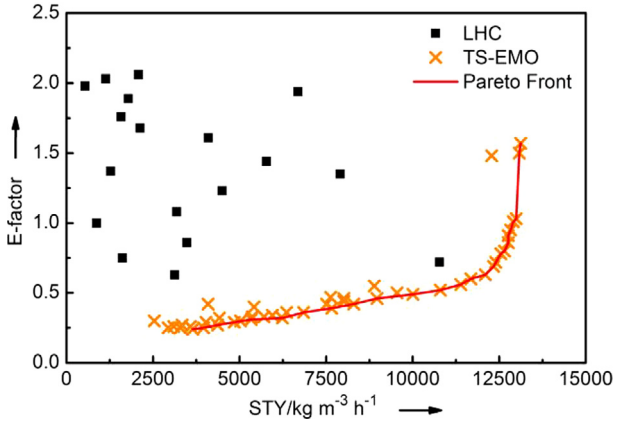

Fig. 2. Results of the four parameter multi-objective self-optimization of the S_NAr reaction (case study one). The initial LHC size was 20. The TS-EMO algorithm conducted 48 additional experiments, 26 of which formed a dense Pareto front highlighting the trade-off between the STY and E-factor. 2 LHC points were omitted for clarity: STY = 370 kg m^{-3} h^{-1}, E-factor = 5.15 & STY = 500 kg m^{-3} h^{-1}, E-factor = 7.07.

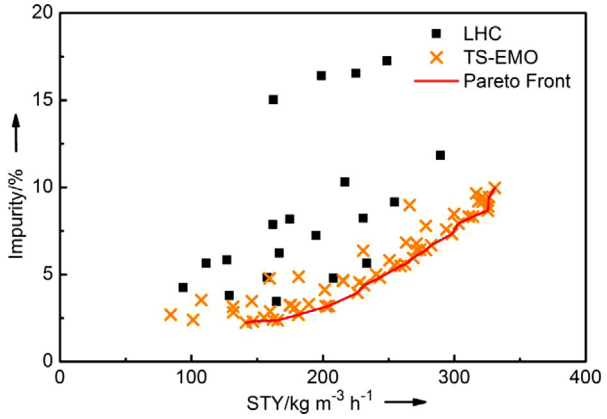

Fig. 3. Results of the four parameter multi-objective self-optimization of the *N*-benzylation (case study two). The initial LHC size was 20. The TS-EMO algorithm conducted 58 additional experiments, 20 of which formed a dense Pareto front highlighting the trade-off between the STY and impurity yield.

in a substantial rise in the E-factor shown by a dramatic increase in the gradient of the Pareto front (operating conditions for each result are provided in the ESI).

As the direct alkylation of amines with alkyl halides is prone to by-product formation via over alkylation [48], we chose the *N*- benzylation of 1° amine **6** as a second case study. *N*,*N*-diisopropylethylamine (DIPEA) was selected as the base for this reaction to suppress the formation of the quaternary ammonium salt [51]. Thus, we aimed to simultaneously maximize the STY of 2° amine **8** and minimize the yield of the 3° amine **9** impurity [Eq. (4)].

$$\text{minimize}\,[-\ln(\text{STY}),\ \ln(\%\,\text{impurity})] \tag{4}$$

As previously, the optimization was conducted with respect to four-variables: **6** flow rate, **7**:**6** ratio, solvent:**6** ratio and temperature (Table 1). The results of the optimization are shown in Fig. 3. Again, the experimental system was run autonomously overnight and was manually terminated in the morning using the same termination criteria as previously.

The results from the initial 20 LHC experiments were better distributed in the objective plane compared to the first case study. Of the 58 experiments designed by the TS-EMO algorithm, 20 points formed a dense Pareto front. The optimal STY was 331 kg m^{-3} h^{-1} with an impurity yield of 10.0%. Conversely, the optimal impurity yield was 2.2% with a STY of 142 kg m^{-3} h^{-1}. Therefore, the data shows the inherent trade-off between STY and % impurity, similar to that observed for the S_NAr reaction between STY and E-factor. Similar to case study one, the STY can initially be increased whilst having a relatively small effect on the % impurity. This corresponds to increasing the concentration of **6** at the lower temperature limits. Any further increase in STY is achieved by increasing the temperature, which results in a substantial increase in the % impurity (operating conditions for each result are provided in the ESI). It should be noted that there was no reduction in reactor performance observed throughout the course of either optimization, indicated by low variability in the results between experiments with similar reaction conditions.

In both case studies, multi-objective optimization successfully identified the target trade-off curve. However, it should be noted that although the proposed algorithm searches globally, stochastic methods cannot give any guarantee that the global Pareto front is approximated to a given tolerance within any finite number of iterations. The main advantage of the Pareto front is that the information it contains can be utilized for process design. For example, it may be beneficial to accept slightly higher impurities in one reaction step if it archives a significantly higher STY that more than offsets the additional downstream processing costs. In contrast, constrained single-objective optimization, such as those used by Reizman [19] and Baumgartner [52], only identify one solution point and reveals no knowledge regarding shape of the Pareto front. In addition, single-objective optimization may find points that are optimal with respect to one objective but that are still dominated by the Pareto front. For instance, Fig. 2 shows several points with a low E-factor and different STY. A single-objective optimization with respect to E-factor cannot differ between those points but the proposed approach identifies points that improve STY without worsening E-factor.

Table 2
Hyperparameters of GP surrogate models. Lower values of θ_i indicate a greater contribution to the objective.

Case Study One: S_NAr Reaction		
Variable	GP 1 (STY)	GP 2 (E-Factor)
$\theta_{\text{residence time}}$	3.02	7.39
$\theta_{\text{morpholine eq.}}$	6.44	5.00
$\theta_{\text{concentration}}$	6.10	0.26
$\theta_{\text{temperature}}$	16.75	1.07
σ_n^2	1.46×10^{-4}	4.54×10^{-5}
Case Study Two: *N*-benzylation		
Variable	GP 1 (STY)	GP 2 (% impurity)
$\theta_{\mathbf{6}}$	13.14	4.20
$\theta_{\mathbf{7:6}}$	11.45	5.53
$\theta_{\text{solvent:}\mathbf{6}}$	20.62	18.11
$\theta_{\text{temperature}}$	7.50	3.28
σ_n^2	4.02×10^{-5}	6.14×10^{-6}

The surrogate models of the underlying objectives include hyperparameters that are provided by the TS-EMO algorithm, which provide qualitative information about the relevance of the input variables. This is referred to as automatic relevance determination [46]. The hyperparameters for both case studies are shown in Table 2. The hyperparameters θ_i correspond to the input variables where lower values indicate a greater contribution to the objective. In the S_NAr case study, the temperature and concentration are significantly more relevant for E-factor compared to STY, however the residence time and morpholine equivalents are relevant to both objectives. This is consistent with the Pareto optimal points, where the residence time and morpholine equivalents are the decisive variables in determining the trade-off between STY and E-factor. In the *N*-benzylation case study, **6** and **7**:**6** are more relevant for the % impurity than for the STY. In contrast to the first case study, the temperature is relevant to both objectives. This is consistent with the Pareto optimal points where temperature is the decisive variable in determining the trade-off between % impurity and STY.

Furthermore, the σ_n^2 hyperparameters correspond to the noise of the system. The low values observed for the systems indicate high quality and consistent data. As a result, we were able to generate precise GP surrogate models of the data, which can be used to predict the response of additional experiments. In the ESI, we show that the GP surrogate models can be further optimized to provide a denser Pareto front. This is useful for the optimization of processes involving high value reagents, where the number of actual experiments is limited by cost/availability.

3. Conclusion

In conclusion, we have demonstrated the application of a machine learning global multi-objective optimization algorithm for the self-optimization of reaction conditions. Two case studies using exemplar reactions have been presented, and the proposed setup was capable of simultaneously optimizing productivity (STY) and environmental impact (E-factor) or % impurity. The four-parameter optimizations

efficiently converged to dense Pareto fronts within 68 and 78 experiments respectively. These revealed the complete trade-off between the objectives, which is valuable information when identifying a good compromise between multiple performance criteria. The developed approach is suitable for any robotic optimization procedure with continuous optimization variables and is readily extended to more than two simultaneous objectives. The use of Gaussian process models provides additional knowledge about the nature of interactions within the system, i.e., the contribution of input variables to the objective functions, as well as numerical characterization of the quality of the experiments.

Conflicts of Interest

There are no conflicts to declare.

Acknowledgments

AMS thanks the Ernest-Solvay-Foundation and the ERASMUS + program for a scholarship for his exchange at the University of Cambridge. AC and NH thank the EPSRC, University of Leeds and AstraZeneca for CASE student funding. The authors would like to thank the editor, Dr. Guy B. B. Marin, and the anonymous reviewers for their valuable feedback towards improving the manuscript.

Appendix A. Supplementary data

Supplementary data associated with this article can be found, in the online version, at https://doi.org/10.1016/j.cej.2018.07.031.

References

[1] C. Houben, A.A. Lapkin, Automatic discovery and optimization of chemical processes, Curr. Opin. Chem. Eng. 9 (2015) 1–7.
[2] S.V. Ley, D.E. Fitzpatrick, R.J. Ingham, R.M. Myers, Organic synthesis: march of the machines, Angew. Chem. Int. Ed. 54 (2015) 3449–3464.
[3] D.C. Fabry, E. Sugiono, M. Rueping, Online monitoring and analysis for autonomous continuous flow self-optimizing reactor systems, React. Chem. Eng. 1 (2016) 129–133.
[4] V. Sans, L. Cronin, Towards dial-a-molecule by integrating continuous flow, analytics and self-optimisation, Chem. Soc. Rev. 45 (2016) 2032–2043.
[5] B.J. Reizman, K.F. Jensen, Feedback in flow for accelerated reaction development, Acc. Chem. Res. 49 (2016) 1786–1796.
[6] D.N. Jumbam, R.A. Skilton, A.J. Parrott, R.A. Bourne, M. Poliakoff, The effect of self-optimisation targets on the methylation of alcohols using dimethyl carbonate in supercritical CO_2, J. Flow Chem. 1 (2012) 24–27.
[7] S. Krishnadasan, R.J.C. Brown, A.J. deMello, J.C. deMello, Intelligent routes to the controlled synthesis of nanoparticles, Lab Chip 7 (2007) 1434–1441.
[8] R.A. Skilton, A.J. Parrott, M.W. George, M. Poliakoff, R.A. Bourne, Real-time feedback control using online attenuated total reflection fourier transform infrared (ATR FT-IR) spectroscopy for continuous flow optimization and process knowledge, Appl. Spectroscopy 67 (2013) 1127–1131.
[9] V. Sans, L. Porwol, V. Dragone, L. Cronin, A self optimizing synthetic organic reactor system using real-time in-line NMR spectroscopy, Chem. Sci. 6 (2015) 1258–1264.
[10] N. Holmes, G.R. Akien, R.J.D. Savage, C. Stanetty, I.R. Baxendale, A.J. Blacker, B.A. Taylor, R.L. Woodward, R.E. Meadows, R.A. Bourne, Online quantitative mass spectrometry for the rapid adaptive optimisation of automated flow reactors, React. Chem. Eng. 1 (2016) 96–100.
[11] J.P. McMullen, K.F. Jensen, An automated microfluidic system for online optimization in chemical synthesis, Org. Process Res. Dev. 14 (2010) 1169–1176.
[12] A.J. Parrott, R.A. Bourne, G.R. Akien, D.J. Irvine, M. Poliakoff, Self-optimizing continuous reactions in supercritical carbon dioxide, Angew. Chem. Int. Ed. 50 (2011) 3788–3792.
[13] J.A. Nelder, R. Mead, A simplex method for function minimization, Computer J. 7 (1965) 308–313.
[14] M.W. Routh, P.A. Swartz, M.B. Denton, Performance of the super modified simplex, Anal. Chem. 49 (1977) 1422–1428.
[15] W. Huyer, A. Neumaier, SNOBFIT – stable noisy optimization by branch and fit, ACM TOMS 35 9 (1–9) (2008) 25.
[16] N. Holmes, G.R. Akien, A.J. Blacker, R.L. Woodward, R.E. Meadows, R.A. Bourne, Self-optimisation of the final stage in the synthesis of EGFR kinase inhibitor AZD9291 using an automated flow reactor, React. Chem. Eng. 1 (2016) 366–371.
[17] D. Cortés-Borda, K.V. Kutonova, C. Jamet, M.E. Trusova, F. Zammattio, C. Truchet, M. Rodriguez-Zubiri, F.-X. Felpin, Optimizing the heck-matsuda reaction in flow with a constraint-adapted direct search algorithm, Org. Process Res. Dev. 20 (2016) 1979–1987.
[18] J.P. McMullen, M.T. Stone, S.L. Buchwald, K.F. Jensen, An integrated microreactor system for self-optimization of a heck reaction: from micro- to mesoscale flow systems, Angew. Chem. Int. Ed. 49 (2010) 7076–7080.
[19] B.J. Reizman, Y.-M. Wang, S.L. Buchwald, K.F. Jensen, Suzuki-Miyaura cross-coupling optimization enabled by automated feedback, React. Chem. Eng. 1 (2016) 658–666.
[20] B.J. Reizman, K.F. Jensen, Simultaneous solvent screening and reaction optimization in microliter slugs, Chem. Commun. 51 (2015) 13290–13293.
[21] A. Echtermeyer, Y. Amar, J. Zakrzewski, A. Lapkin, Self-optimisation and model-based design of experiments for developing a C-H activation flow process, Beilstein J. Org. Chem. 13 (2017) 150–163.
[22] R.A. Bourne, R.A. Skilton, A.J. Parrott, D.J. Irvine, M. Poliakoff, Adaptive process optimization for continuous methylation of alcohols in supercritical carbon dioxide, Org. Process Res. Dev. 15 (2011) 932–938.
[23] R.A. Skilton, R.A. Bourne, Z. Amara, R. Horvath, J. Jin, M.J. Scully, E. Streng, S.L.Y. Tang, P.A. Summers, J. Wang, E. Pérez, N. Asfaw, G.L.P. Aydos, J. Dupont, G. Comak, M.W. George, M. Poliakoff, Remote-controlled experiments with cloud chemistry, Nat. Chem. 7 (2015) 1–5.
[24] J.S. Moore, K.F. Jensen, Automated multitrajectory method for reaction optimization in a microfluidic system using online IR analysis, Org. Process Res. Dev. 16 (2012) 1409–1415.
[25] C. Houben, N. Peremezhney, A. Zubov, J. Kosek, A.A. Lapkin, Closed-loop multi-target optimization for discovery of new emulsion polymerization recipes, Org. Process Res. Dev. 19 (2015) 1049–1053.
[26] N. Peremezhney, E. Hines, A. Lapkin, C. Connaughton, Combining Gaussian processes, mutual information and a genetic algorithm for multi-target optimization of expensive-to-evaluate functions, Eng. Optimiz. 46 (2014) 1593–1607.
[27] D.E. Fitzpatrick, C. Battilocchio, S.V. Ley, A novel internet-based reaction monitoring, control and autonomous self-optimization platform for chemical synthesis, Org. Process Res. Dev. 20 (2016) 386–394.
[28] K. Deb, K. Sindhya, J. Hakanen, Decision Sciences: Theory and Practice, CRC Press, 2016, pp. 145–184.
[29] S.M. Aworinde, A.M. Schweidtmann, A.A. Lapkin, The concept of selectivity control by simultaneous distribution of the oxygen feed and wall temperature in a microstructured reactor, Chem. Eng. J. 331 (2018) 765–776.
[30] M. Xu, S. Bhat, R. Smith, G. Stephens, J. Sadhukhan, Multi-objective optimisation of metabolic productivity and thermodynamic performance, Comp. Chem. Eng. 33 (2009) 1438–1450.
[31] A. Tarafder, G.P. Rangaiah, A.K. Ray, Multiobjective optimization of an industrial styrene monomer manufacturing process, Chem. Eng. Sci. 60 (2005) 347–363.
[32] D. Sarkar, J.M. Modak, Pareto-optimal solutions for multi-objective optimization of fed-batch bioreactors using nondominated sorting genetic algorithm, Chem. Eng. Sci. 60 (2005) 481–492.
[33] S. Garg, S.K. Gupta, Multiobjective optimization of a free radical bulk polymerization reactor using genetic algorithm, Macromol. Theory Simul. 8 (1999) 46–53.
[34] K. Ulonska, A. König, M. Klatt, A. Mitsos, J. Viell, Optimization of multiproduct biorefinery processes under consideration of biomass supply chain management and market developments, Ind. Eng. Chem. Res. 57 (2018) 6980–6991.
[35] D. Helmdach, P. Yaseneva, P.K. Heer, A.M. Schweidtmann, A.A. Lapkin, A multi-objective optimisation including results of life cycle assessment in developing bio-renewables-based processes, ChemSusChem 10 (2017) 3632–3643.
[36] V. Bhaskar, S.K. Gupta, A.K. Ray, Applications of multiobjective optimization in chemical engineering, Rev. Chem. Eng. 16 (2000) 1–54.
[37] A.I.J. Forrester, A.J. Keane, Recent advances in surrogate-based optimization, Prog. Aerosp. Sci. 45 (2009) 50–79.
[38] B. Shahriari, K. Swersky, Z. Wang, R.P. Adams, N. de Freitas, Taking the human out of the loop: a review of bayesian optimization, Proc. IEEE 104 (2016) 148–175.
[39] F. Boukouvala, R. Misener, C.A. Floudas, Global optimization advances in mixed-integer nonlinear programming, MINLP, and constrained derivative-free optimization, CDFO, Eur. J. Oper. Res. 252 (2016) 701–727.
[40] E. Bradford, A.M. Schweidtmann, A. Lapkin, Efficient multiobjective optimization employing Gaussian processes, spectral sampling and a genetic algorithm, J. Global Optim. 71 (2018) 407–438.
[41] E. Bradford, A.M. Schweidtmann, A. Lapkin, Correction to: efficient multiobjective optimization employing Gaussian processes, spectral sampling and a genetic algorithm, J. Global Optim. 71 (2018) 439–440.
[42] E. Bradford, A. M. Schweidtmann, A. Lapkin, TS-EMO, GitHub. (2018). https://github.com/Eric-Bradford/TS-EMO (accessed June 22, 2018).
[43] J. Knowles, ParEGO: a hybrid algorithm with on-line landscape approximation for expensive multiobjective optimization problems, IEEE Trans. Evol. Comput. 10 (2006) 50–66.
[44] M. Emmerich, Single-and multi-objective evolutionary design optimization assisted by Gaussian random field metamodels. Ph.D. thesis, University of Dortmund (2005).
[45] V.R. Joseph, Y. Hung, Orthogonal-maximin latin hypercube designs, Statistica Sinica 18 (2008) 171–186.
[46] C.E. Rasmussen, C.K.I. Williams, Gaussian Processes for Machine Learning (Adaptive Computation and Machine Learning), MIT Press, 2005.
[47] A.G. O'Brien, Z. Horváth, F. Lévesque, J.W. Lee, A. Seidel-Morgenstern, P.H. Seeberger, Continuous synthesis and purification by direct coupling of a flow reactor with simulated moving-bed chromatography, Angew. Chem. Int. Ed. 51 (2012) 7028–7030.
[48] R.N. Salvatore, C.H. Yoon, K.W. Jung, Synthesis of secondary amines, Tetrahedron 57 (2001) 7785–7811.

[49] R.A. Sheldon, Organic synthesis; past, present and future, Chem. Ind. 903–906 (1992).
[50] D.R. Jones, M. Schonlau, W.J. Welch, Efficient global optimization of expensive black-box functions, J. Global Optim. 13 (1998) 455–492.
[51] J.L. Moore, S.M. Taylor, V.A. Soloshonok, An efficient and operationally convenient general synthesis of tertiary amines by direct alkylation of secondary amines with alkyl halides in the presence of Huenig's base, Arkivoc 6 (2005) 287–292.
[52] L.M. Baumgartner, C.W. Coley, B.J. Reizman, K.W. Gao, K.F. Jensen, Optimum catalyst selection over continuous and discrete process variables with a single droplet microfluidic reaction platform, React. Chem. Eng. 3 (2018) 301–311.